Simulated Physical Mechanisms Associated with Climate Variability over Lake Victoria Basin in East Africa

RICHARD O. ANYAH

Center for Environmental Prediction, Department of Environmental Sciences, Rutgers, The State University of New Jersey, New Brunswick, New Jersey

FREDRICK H. M. SEMAZZI

Department of Marine, Earth and Atmospheric Sciences, and Department of Mathematics, North Carolina State University, Raleigh, North Carolina

LIAN XIE

Department of Marine, Earth and Atmospheric Sciences, North Carolina State University, Raleigh, North Carolina

(Manuscript received 5 October 2005, in final form 21 March 2006)

ABSTRACT

A fully coupled regional climate, 3D lake modeling system is used to investigate the physical mechanisms associated with the multiscale variability of the Lake Victoria basin climate. To examine the relative influence of different processes on the lake basin climate, a suite of model experiments were performed by smoothing topography around the lake basin, altering lake surface characteristics, and reducing or increasing the amount of large-scale moisture advected into the lake region through the four lateral boundaries of the model domain. Simulated monthly mean rainfall over the basin is comparable to the satellite (Tropical Rainfall Measuring Mission) estimates. Peaks between midnight and early morning hours characterize the simulated diurnal variability of rainfall over the four quadrants of the lake, consistent with satellite estimates, although the simulated peaks occur a little earlier. It is evident in the simulations with smoothed topography that the upslope/downslope flow generated by the mountains east of the lake and the land–lake breeze circulations play important roles in influencing the intensity, the location of lake/land breeze fronts, and the horizontal extent of the land–lake breeze circulation, as well as lake basin precipitation. When the lake surface is replaced with marsh (water hyacinth), the late night and early morning rainfall maximum located over the western sector of the lake is dramatically reduced. Our simulations also indicate that large-scale moisture transported via the prevailing easterly trades enhances lake basin precipitation significantly. This is in contrast to the notion advanced in some of the previous studies that Lake Victoria generates its own climate (rainfall) through precipitation–evaporation–reprecipitation recycling only.

1. Introduction

The primary objective of the present study is to characterize and understand the relative roles of several physical mechanisms associated with the coupled lake–atmosphere climate variability over Lake Victoria basin in East Africa on diurnal through interannual time scales. Lake Victoria basin is one of the agriculturally productive areas in East Africa and thus a major breadbasket for the region. Besides having an agriculturally rich hinterland, the lake also supports and sustains important fisheries, maintains an energy supply (hydroelectric power), and is a potent source of both domestic and industrial water supply. The lake is also one of the primary sources of the river Nile (the longest river in the world), which could be viewed as the hydrological "placenta" and lifeline of semiarid countries downstream, which include the Sudan, Ethiopia, and Egypt.

Lake Victoria basin, situated within a shallow continental sag between the two arms of the East Africa

Corresponding author address: Dr. Richard Anyah, Center for Environmental Prediction, Department of Environmental Sciences, Rutgers, The State University of New Jersey, New Brunswick, NJ 08901.
E-mail: anyah@cep.rutgers.edu

Great Rift Valley system (Fig. 1), provides an environment conducive for complex interactions and integrations between regionally induced and large-scale circulation systems. These include topographic and lake-induced circulations (Song et al. 2004; Anyah and Semazzi 2004), circulations associated with widespread variations in land cover/land use characteristics, monsoonal circulations associated with the thermal contrast between land and the nearby Indian Ocean (Okeyo 1987; Mukabana and Pielke 1996), and the influence of the humid Congo air mass emanating from the tropical (Congo) rain forest (Anyamba 1984; Sun et al. 1999a).

The general climate of the lake basin ranges from a modified equatorial type with substantial rainfall occurring throughout the year, particularly over the lake and its vicinity, to a semiarid type characterized by intermittent droughts over some areas located even within short distances from the lakeshore. However, the seasonal rainfall is characterized by a bimodal regime: March–May and October–December, locally known as *long* and *short* rainy seasons, respectively. During the short rainy season, rainfall is more widespread over the entire lake basin during the month of November (Asnani 1993). The seasonal cycle of rainfall is mainly controlled by the north–south migration of the intertropical convergence zone (ITCZ) across the region, whereas the diurnal cycle is dominated by lake/land breeze circulations. Large-scale precipitation over the lake basin is mainly initiated from the southeastern (eastern) Indian Ocean monsoon flow that transports maritime moisture into the interior of East Africa. The humid Congo air mass also significantly boosts convection and overall rainfall amounts received over the western and northwestern parts of the lake (Anyamba 1984). However, a quasi-permanent trough that lingers over Lake Victoria (Asnani 1993) due to locally induced convection, orographic influence, and land–lake thermal contrast tends to favor convection over the lake basin throughout the year. In terms of interannual variability, the Lake Victoria basin climate is characterized by periodic episodes of anomalously wet or dry conditions associated with SST anomalies over equatorial Indian Ocean (e.g., 1961 floods) and also Pacific Ocean SST perturbations (e.g., 1997/98 ENSO-related floods).

However, the complex interactions between regional and large-scale processes and their associated modulating influence on the regional climate are not yet well investigated quantitatively. Furthermore, many previous investigators have primarily used empirical methods that are based mainly on the scarce observations over the region and thus do not offer adequate scope to sufficiently unveil the cause–effect relationships between regional climate variability and an individual process or combination of processes. Such cause–effect relationships may only be understood through the numerical modeling approach that also accounts for the lake–atmosphere coupled variability. Hence, in the present study, we have applied a fully coupled regional climate–three-dimensional lake modeling system–Princeton Ocean Model (RegCM3–POM; Song et al. 2002, 2004; Blumberg and Mellor 1987; Anyah 2005) to investigate how the interactions among local and large-scale factors (processes) modulate the Lake Victoria basin climate. A coupled modeling system provides a rich test bed for examining the response of the lake basin (and regional climate) to an individual process or a combination of processes through a suite of systematic sensitivity simulations.

We investigate the role of complex topography (steep terrain on both sides of the lake) and whether it helps to organize, enhance, and/or suppress the development of convective activity over the lake basin and surrounding areas. Also, we have examined how changes in lake surface characteristics, as typified by the invasion of a large swath of the lake surface by water hyacinth weed, alters the lake–atmosphere interactions and eventually the lake basin climate. In addition, experiments are performed to investigate the extent to which large-scale moisture transported via the prevailing monsoonal flows affects the overall climate (rainfall pattern) over the lake basin. We focus on the short rains due to the large spatial and temporal variability of rainfall experienced during this season compared to the long rainy season (Nicholson 1996). As a result, the regional climate during the short rains is highly sensitive to perturbations in both large- and local-scale climate systems (Sun et al. 1999a).

Mesoscale lake-effect circulations have been shown to develop through complex interactions of an array of environmental and geographic variables such as lake–air temperature differences, wind speed, lower-tropospheric stability, lake shape, or bathymetry (Laird et al. 2003a,b). McPherson (1970) established that the distribution of the thermal surface gradient (i.e., caused by shoreline configuration) and interaction with the ambient wind may enhance or diminish the low-level convergence and vertical circulation within the lake basins. This is consistent with the study by Hostetler and Giorgi (1992), who noted that increased simulated precipitation in the presence of large inland lakes was due to an increase in overlake evaporation that adds water vapor to the prevailing flow systems, thereby enhancing convective instability and precipitation associated with such systems. This is more pronounced when the lake

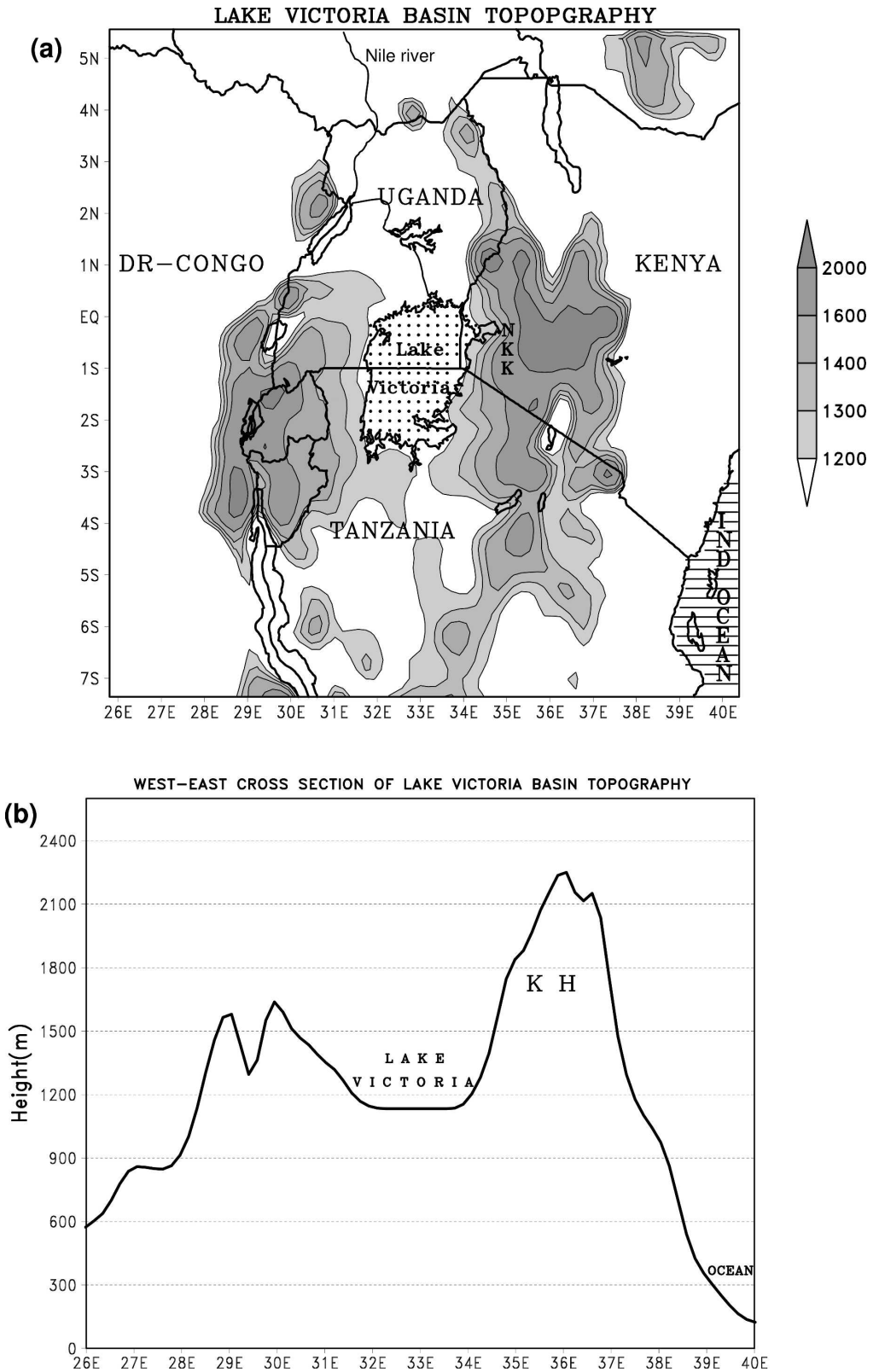

FIG. 1. (a) Terrain height around Lake Victoria basin; areas higher than 1200 m are shaded (NKK highlands). (b) Horizontal cross section of the elevation around Lake Victoria basin along 1°S (KH represents Kenya highlands).

surface temperatures are much warmer than the overlying atmosphere.

Fraedrich (1972) made a significant contribution to the understanding of this problem over Lake Victoria in East Africa by investigating the dynamics of nocturnal circulations and the frequent development of thunderstorms over the northwestern/western sector(s) of the lake using an analytical (climatological) model. The dynamical processes linked to the nocturnal circulation patterns were found in this study to be associated with three-way interactions among the diurnal land–lake breeze circulations, the upslope or downslope mountain or valley winds, and prevailing (large scale) monsoonal flow. The resultant "nonlinear" interactions favor strong convergence over the western sector of the lake at night but over land areas east of the lake catchment during the day (Okeyo 1987). The diurnal and monthly rainfall variability is also closely linked with this flow pattern (Mukabana and Pielke 1996), with the western sector receiving more rainfall than the eastern sector in terms of the monthly mean totals. Asnani (1993) also showed that rainfall over the lake is about 30%–35% more than over the surrounding land areas. Ba and Nicholson (1998) also used satellite data and showed that the frequency of cold cloud duration over the lake is about 25%–30% greater than over the surrounding land, although the estimated overlake rainfall pattern was found to be highly correlated with basinwide rainfall (Mistry and Conway 2003). Thus, it is unlikely that causes of the dramatic lake level fluctuations experienced during the 1961 and 1997/98 flood episodes over the region can be well understood without accounting for the contribution from large-scale forcing to regional rainfall variability. After all, the bimodal rainfall pattern associated with the passage of the ITCZ across eastern Africa is also well marked in the overlake rainfall variability (Nicholson 1998; Mistry and Conway 2003), indicating that the rainfall pattern over the lake basin is also partly driven by fluctuations in the large-scale climatic conditions.

Recently, Song et al. (2002, 2004) developed a fully coupled regional climate modeling system (RegCM2–POM) to simulate the coupled lake–atmosphere climate variability over Lake Victoria basin. They demonstrated that adopting the traditional modeling approach in which the three-dimensional lake hydrodynamics and thermodynamics are neglected, as in cases where the lake is represented by a simple 1D thermal equation (Sun et al. 1999b; Anyah and Semazzi 2004), is not entirely satisfactory for Lake Victoria. Their results further demonstrated that the fully coupled RegCM2–3D model simulated more realistic climate conditions over eastern Africa and Lake Victoria basin compared to observations and results from the standard RegCM2–1D model adopted in Hostetler et al. (1993), Sun et al. (1999b) and Anyah and Semazzi (2004).

In the present study, the response of lake basin and regional climate to nonlinear interactions among topographic-induced circulations, land–lake breeze circulations, and large-scale (prevailing) monsoonal flow is investigated based on an enhanced and improved version of the RegCM3–3D lake modeling system (Anyah 2005). Additionally, the impacts of changes in the physical characteristics of the lake surface (as exemplified with a recent invasion of a large swath of the lake by water hyacinth) on the lake and basinwide climate variability are examined. A brief description of the coupled modeling system and the design of numerical experiments is given in section 2. Results and discussions are presented in section 3, while the summary and conclusions are given in section 4.

2. Description of component models of the RegCM3–POM system

a. RegCM3 model

RegCM3 is a three-dimensional primitive equation atmospheric model (Pal et al. 2005, manuscript submitted to *Bull. Amer. Meteor. Soc.*). It is an improved and augmented version of the National Center for Atmospheric Research (NCAR) RegCM2 (Giorgi et al. 1993a,b). The model uses a terrain-following (sigma pressure) vertical coordinate system. The radiation physics calculations are based on the NCAR Community Climate Model version 3 (CCM3) GCM radiation scheme (Kiehl et al. 1996) that includes a component for computing the effects of greenhouse gases (NO_2, CH4, and CFCs), aerosols, and cloud ice. The land surface physics parameterizations are based on the Biosphere–Atmosphere Transfer Scheme version 1e (BATS1e: Dickinson et al. 1993) in which a standard surface drag coefficient based on surface-layer similarity theory is applied to calculate sensible heat, water vapor (latent heat), and momentum fluxes.

Two major enhancements in the cloud and precipitation processes have been implemented in RegCM3 since its earlier version, RegCM2. First, moisture is prognosticated based on cloud water formation, advection and mixing by turbulence, and reevaporation and conversion of cloud water into rain via a bulk autoconversion term. Second, the large-scale precipitation parameterization, subgrid explicit moisture scheme (SUBEX; Pal et al. 2000), is used to account for nonconvective clouds and model-resolved precipitation. SUBEX accounts for the subgrid variability in clouds

by relating the average gridcell relative humidity to cloud fraction and cloud water based on the formulation by Sundqvist et al. (1989).

Further modifications and customization of RegCM3 for the equatorial eastern Africa domain were carried out at North Carolina State University's Climate Simulation Laboratory (Anyah 2005). These followed the criteria applied in Sun et al. (1999a,b) during the first application of NCAR RegCM2 for simulating the region's climate and in Song et al. (2002) during the initial development of a coupled RegCM2–POM system for Lake Victoria basin.

b. *Three-dimensional Lake Victoria model based on POM*

The Princeton Ocean Model (Blumberg and Mellor 1987) is a three-dimensional, nonlinear primitive equation, finite difference ocean model. The model uses a mode splitting technique to solve for the 2D barotropic mode of the free surface currents and the 3D baroclinic mode associated with the full three-dimensional temperature, turbulence, and current structure. The barotropic mode uses a shorter time step, while the baroclinic mode uses a relatively longer time step. Both modes are constrained by the Courant–Friedrichs–Lewy (CFL) computational stability criteria. The model is based on a split-explicit Eulerian scheme in which the internal and external modes are integrated separately to optimize computational efficiency. The model includes a 2.5 turbulence closure submodel (Mellor and Yamada 1974) with an implicit time scheme for vertical mixing. The equation of state (Mellor 1991) is used to calculate density as a function of temperature, pressure, and salinity. POM is currently one of the most widely used ocean models and has also been extensively used for studying coastal estuaries and inland lake basins. A detailed description of POM can be found in Blumberg and Mellor (1987). Modifications made to the POM used in this study for freshwater Lake Victoria can be found in Song et al. (2002, 2004) and Anyah (2005). The coupling of the atmosphere and the lake is through the fluxes of momentum, sensible heat, longwave radiation, moisture, latent heat, and shortwave radiation (Fig. 2), and details are available in Song et al. (2004).

c. *Design of numerical experiments*

We first performed RegCM3 model runs over a relatively larger domain covering 15°N–8°S, 10°–55°E, at a spatial resolution of 60 km (i.e., Big Brother Experiments) for the short rains seasons over a 5-yr period (1998–2002). The initial and boundary conditions were taken from the 6-hourly National Centers for Environmental Prediction (NCEP) reanalysis (Kalnay et al. 1996). In these experiments, a simple 1D lake model represented Lake Victoria. For the lake basin experiments with the RegCM3–3D lake modeling system, the model domain covered 5°N–7°S, 25°E–41°E, which encompasses the whole of the Lake Victoria catchment. The initial and boundary conditions were derived from the 6-hourly output of the Big Brother Experiments.

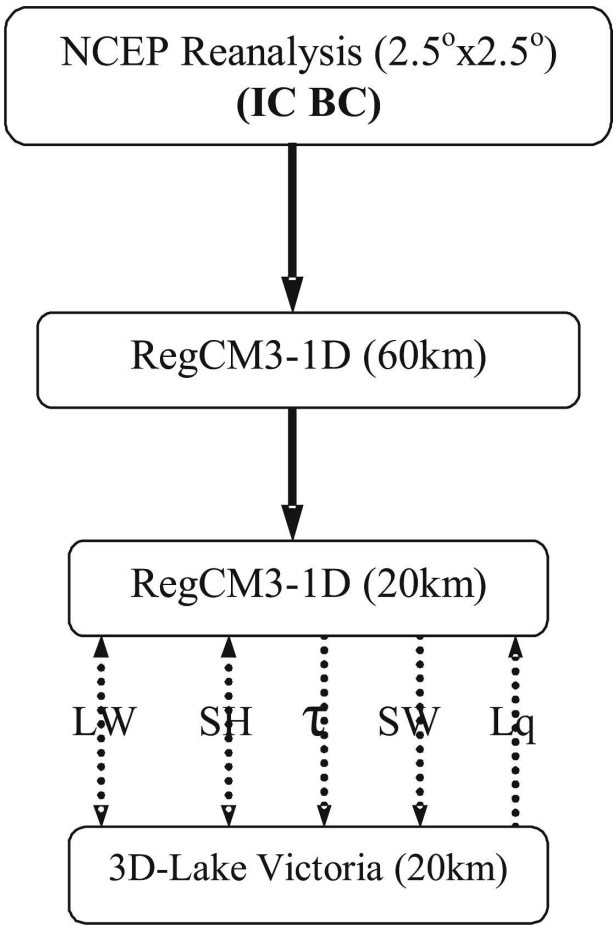

FIG. 2. Schematic of the coupled atmosphere–lake system (modified from Song et al. 2004; LW represents longwave radiation, SW is shortwave radiation, τ is wind stress, Lq is latent heat, and SH is sensible heat).

The physical mechanisms associated with interactions between the lake and regional topography were investigated by performing the following experiments:

- Experiment 1 (CTRL): Control case in which the terrain and land surface/land use characteristics are unaltered.
- Experiment 2 (TPALL): Land surface/land use characteristics are as in CTRL, except the terrain height all around the lake basin is smoothed such that the maximum height is 1300 m above mean sea level

(AMSL) and is just above the approximate lake surface elevation (~1200 m).
- Experiment 3 (TPEA): Same as in TPALL, except only the terrain between the lake and Indian Ocean is smoothed.
- Experiment 4 (LBOG): Similar to CTRL, except the lake is replaced with bog/marsh (swamp) in order to examine the basinwide climate response to changes in lake surface characteristics. We believe that this experiment mimics the ongoing changes in the lake surface characteristics imposed by the invasion of a large swath of the lake surface by water hyacinth.

Seven additional experiments were performed to investigate the role that large-scale moisture transported via the four lateral boundaries of our model domain (covering Lake Victoria basin) plays in the overall lake basin rainfall variability.

- Experiment 5 (Qe-20): Large-scale moisture [mixing ratio (q)] along the eastern lateral boundary is reduced by 20%. This means that the incoming large-scale moisture through the eastern boundary is relatively drier than in the control case. This is done prior to interpolating the boundary and initial conditions onto the model grids in order to avoid any inconsistencies in the physics and dynamics of the model during integrations.
- Experiment 6 (Qe-50): Same as in Qe-20, except large-scale moisture is 50% drier than in the control.
- Experiment 7 (Qe-80): Same as in Qe-20, except large-scale moisture is 80% drier than in the control.
- Experiment 8 (Qw-50): Same as in Qe-50, except large-scale moisture forcing over the western boundary is 50% drier than in the control.
- Experiment 9 (Qs-50): Same as in Qe-20, except large-scale moisture forcing over the southern boundary is 50% drier than in the control.
- Experiment 10 (Qn-50): Same as in Qe-20, except large-scale moisture forcing over the northern boundary is 50% drier than in the control.
- Experiment 11 (Qa-50): Same as in Qe-20, except large-scale moisture forcing over all four lateral boundaries is 50% drier than in the control.

3. Results and discussion

a. Comparison of simulated and satellite rainfall

The RegCM3–3D lake coupled model-simulated diurnal, seasonal, and interannual variability of rainfall are mainly evaluated using the National Aeronautics and Space Administration (NASA) Tropical Rainfall Measuring Mission (TRMM) satellite estimates (available online at http://disc.gsfc.nasa.gov/data/datapool/TRMM_DP/). TRMM data over the lake are currently some of the most comprehensive observational surrogates available for evaluating overlake simulated rainfall because of the lack of high-resolution in situ observations. The precipitation radar aboard the TRMM Microwave Imagery (TMI) satellite is also capable of detecting below-cloud rainfall and is thus a suitable tool for estimating rainfall over Lake Victoria that has a strong diurnal cycle of cloud cover (Kummerow et al. 2000; Ba and Nicholson 1998).

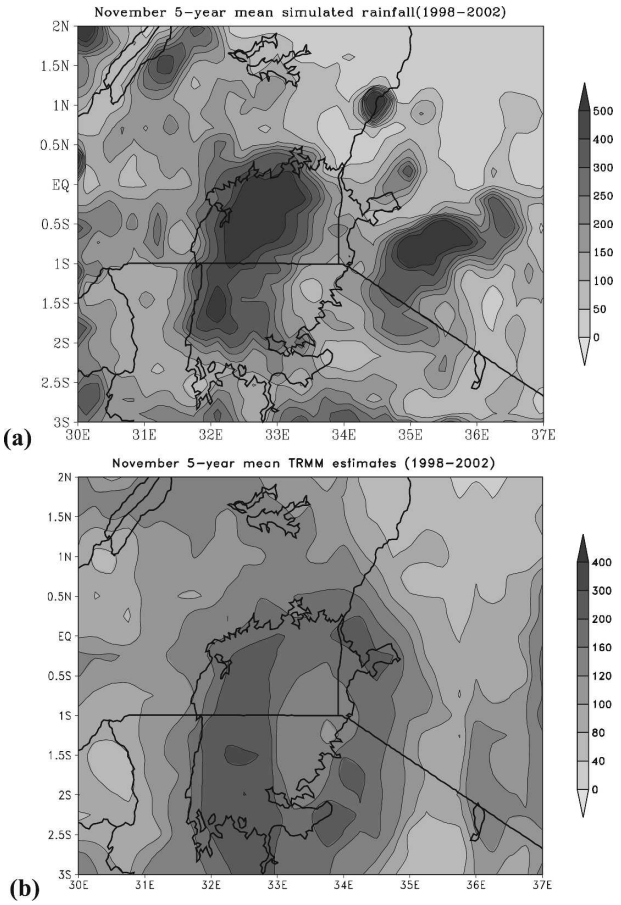

FIG. 3. Five-year rainfall average in November (1998–2002) for the (a) RegCM3–POM simulation and (b) TRMM.

The 5-yr average (1998–2002) of the simulated rainfall in November is compared to TRMM estimates averaged over the same period and is presented in Fig. 3. On the other hand, in Figs. 4a,b, 4c,d, and 4e,f, the simulated and TRMM rainfall are compared in November 1998, 2000, and 2002, respectively. These three years represent periods with relatively different large-scale climatic regimes. The November 1998 short rains season coincided with the mature phase of La Niña conditions, while November 2002 coincided with mod-

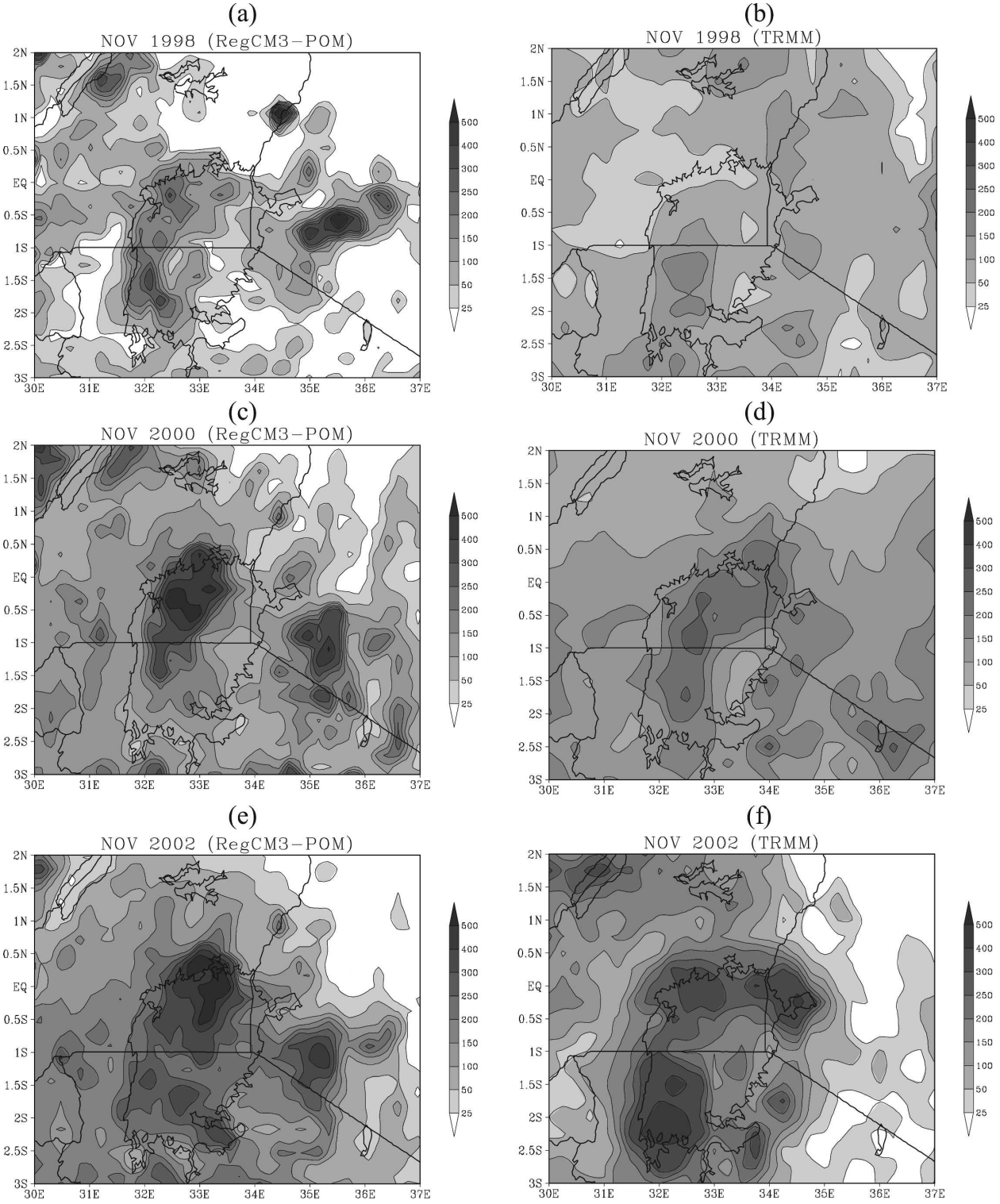

FIG. 4. Comparison between RegCM3–POM simulated monthly mean rainfall and TRMM estimates over Lake Victoria basin in November (a) 1998 model, (b) 1998 TRMM, (c) 2000 model, (d) 2000 TRMM, (e) 2002 model, and (f) 2002 TRMM.

erate El Niño conditions. We treat November 2000 as a near-"normal" season over our study area. Furthermore, the month of November, which is the middle of the short rains season, is generally associated with more widespread rainfall over the lake basin (Asnani 1993), and thus the rainfall characteristics during the month are nearly representative of the overall rainfall pattern and/or fluctuations during the entire season.

In November 1998 (Figs. 4a,b), the model generally simulates more rainfall over the entire lake basin compared to the TRMM. Large amounts of rainfall are simulated over the western and northwestern sectors of the lake, with the maximum peak located slightly to the southwest. The TRMM rainfall maximum is located over the southwestern section of the lake surface as well, although the peak amount is about 180 mm compared to over 280 mm simulated by the model, a difference of about 50%. In addition, the model simulations show a secondary region of enhanced rainfall to the east of the lake (approximately located over the Nandi-Kericho-Kisii (NNK) highlands; see Fig. 1), which is conspicuously missing in the TRMM estimates. Since 1998 was the first year of the TRMM mission, it has been noted that many errors in the algorithms used in computing satellite rainfall estimates had not been corrected (Kummerow et al. 2000). However, the inability of the RegCM3–POM coupled model to adequately resolve rainfall over the elevated regions east of Lake Victoria may also be associated with the model's relatively coarse spatial resolution (20 km) as well as a deficiency in the model's precipitation physics, leading to unrealistically high amounts of simulated rainfall.

In Figs. 4c,d, both the simulated and TRMM rainfall in November 2000 are characterized by higher rainfall amounts over the western and northwestern sector of the lake compared to the surrounding areas. In addition, the overall simulated rainfall pattern is reasonably consistent with the TRMM estimates (Fig. 4c). However, the simulated rainfall pattern and amount is not in good agreement with TRMM estimates over the highlands east of the lake. The exceptionally high amounts of rainfall simulated are likely due to the deficiency of the model dynamics/physics in capturing the rainfall pattern over the high terrain east of the lake at the present spatial resolution of 20 km. But the relatively dry conditions (less rainfall) simulated over the hinterlands to the west of the lake qualitatively agree with the low values seen in the TRMM estimates.

Figures 4e,f shows that the simulated rainfall in November 2002 over the northern and northwestern quadrant of the lake surface is in general agreement with TRMM estimates, in terms of both the location of rainfall maximum as well as the spatial distribution. However, significant differences are evident between simulated and TRMM rainfall over the southwestern sector of the lake. TRMM rainfall estimates over the southwestern part of the lake surface are relatively higher than the simulated amount by over 50%. However, the simulated dry conditions over the land areas northeast of the lake catchment are consistent with the TRMM estimates (Fig. 4f).

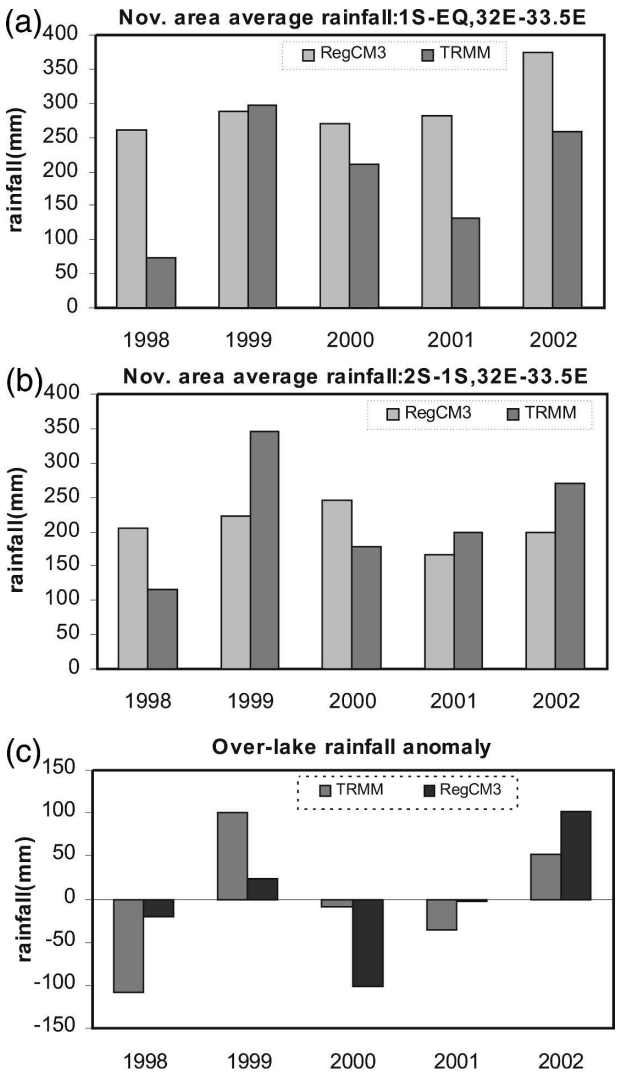

FIG. 5. Overlake averaged rainfall in the (a) northern and (b) southern half, and (c) overlake rainfall anomaly based on the 1998–2002 average.

In Figs. 5a,b, the simulated area-averaged rainfall over the northern half of the lake (0°–1°S) and the southern half (1°–2°S) are compared with the TRMM estimates. Over the northern half of the lake, the model overestimates the rainfall total in four out of the five years (i.e., 1998, 2000, 2001, and 2002) compared to

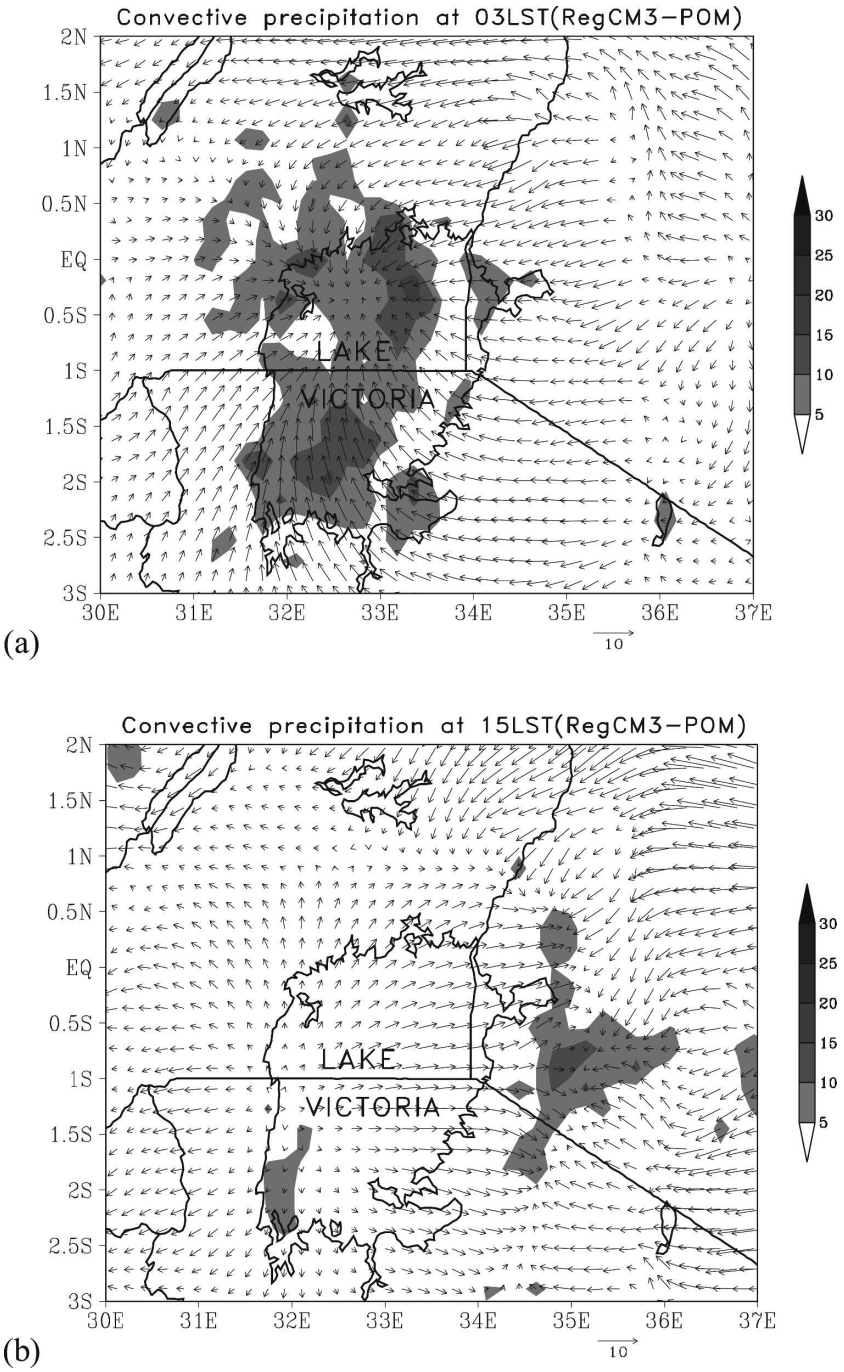

FIG. 6. Overlay of 850-hPa mean flow on convective precipitation over the lake basin at (a) 0300 and (b) 1500 LST.

TRMM estimates. On the other hand, over the southern half, the simulated rainfall totals are lower than the TRMM rainfall for three out of the five years (i.e., 1999, 2001, and 2002). However, the model and TRMM are in relatively better agreement over the southern half of the lake compared to the northern half. The negative differences between the model and TRMM over both halves in November 1998 (La Niña) are generally consistent with previous studies, which have shown that during La Niña events, most parts of East Africa including the lake basin tend to experience below normal rainfall amounts (e.g., Ogallo 1988; Nicholson 1996). This is also apparent in Fig. 5c, which shows the anomaly of the overlake rainfall based on a 5-yr (1998–

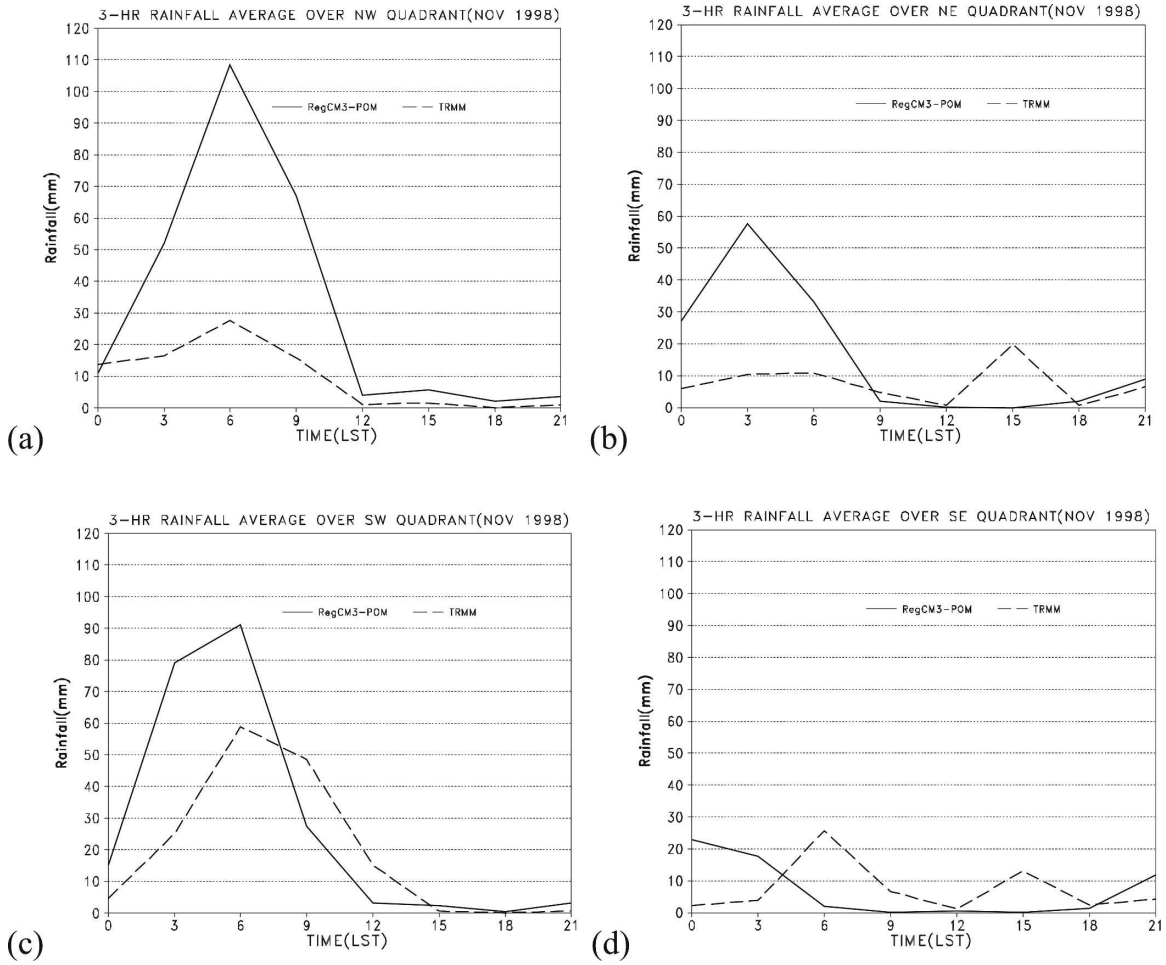

FIG. 7. Three-hourly total rainfall over four different quadrants over the lake in November 1998.

2002) mean. Both simulated and satellite (TRMM) estimated anomalies are negative, although the anomaly in the satellite estimate is relatively larger.

Overall, the coupled RegCM3–POM reasonably reproduces the spatial and temporal variability of Lake Victoria basin rainfall (Figs. 3–5), which is consistent with TRMM satellite estimates. It is, however, clearly evident that during all 5 yr covered by our simulations, the simulated overlake rainfall amounts are higher than over the surrounding land areas by almost 30%–50%. This is consistent with TRMM estimates, although the simulated values are much more exaggerated.

b. Diurnal cycle of circulation and precipitation over Lake Victoria

The mean circulation pattern and associated land or lake breeze circulation driven convection (convective precipitation) is given in Fig. 6. The peak of the nocturnal circulation generally occurs between midnight and early morning hours, when the lake surface is much warmer than the surrounding land areas (Fraedrich 1972). Conversely, the peak lake breeze circulation occurs between late afternoon and early evening (Okeyo 1987), when the adjoining land surface is much warmer than the lake surface. Figure 6a shows the simulated mean circulation pattern in the morning at 0300 LST for the month of November. The circulation pattern over the lake basin is characterized by flow convergence over the western sector of the lake consistent with previous studies (e.g., Fraedrich 1972; Okeyo 1987; Datta 1981; Song et al. 2002).

Figure 6b shows the mean circulation pattern over the lake basin at 15 LST, when the lake breeze circulation is expected to be fully developed. The model clearly captures outflow from the lake surface and the apparent location of the lake breeze front east of the lake, around 35°E. However, the exact location of the land breeze (nocturnal circulation) front is not clearly resolved in the model simulations. The simulated land breeze circulation is also relatively weaker and the ap-

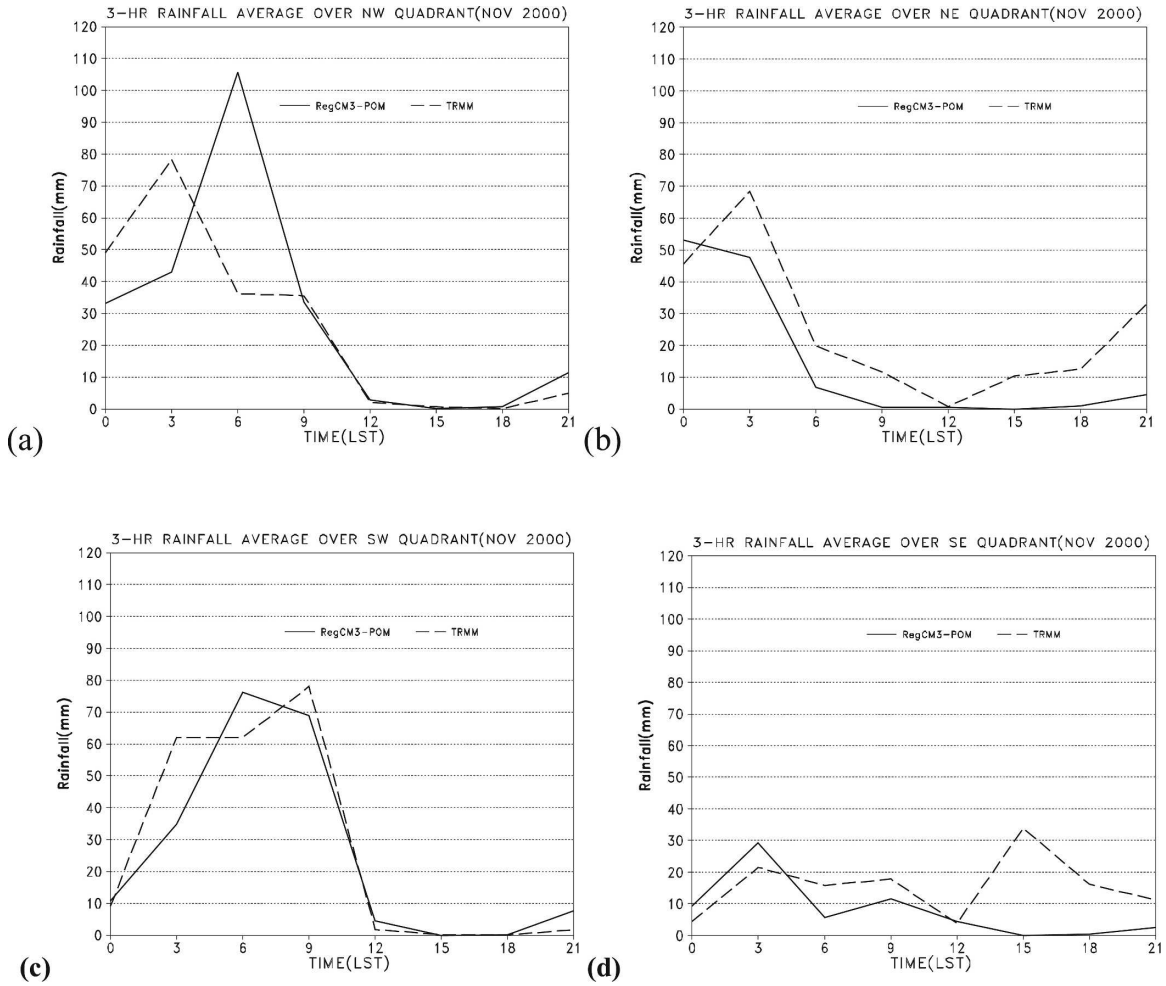

FIG. 8. Same as in Fig. 7, but for November 2000.

proximate location of the land breeze front is confined within the western rim of the lake surface. It is also important to note that Lake Victoria forms a quasi-permanent trough and is surrounded by high mountain ranges on both sides, thus, often the statically stable air over the lake during the day partly determines the intensity of the lake breeze circulation. The simulated convective precipitation associated with the times of peak land–lake breeze is consistent with the simulated circulation patterns. It can be seen that a significant amount of rainfall is simulated over the western sector of the lake around 3 LST, but outside the lake surface over the land areas and east of the lake basin (over the NNK highlands; Fig. 1) around 15 LST.

Figures 7, 8, and 9 show the total simulated and TRMM estimated diurnal rainfall variability over four different quadrants of the lake surface for November 1998, November 2000, and November 2002, respectively. The four quadrants are $1° \times 1°$ square boxes ($\sim$10,000 km^2) over the lake surface and are designated as northwest quadrant (NW: 0°–1°S, 32°E 33°E), southwest quadrant (SW: 1°–2°S, 32°E–33°E), northeast quadrant (NE: 0°–1°S, 33°E–34°E), and southeast quadrant (SE: 1°–2°S, 33°E 34°E). We use 3-h rainfall totals to derive the diurnal cycles since the TRMM estimates were not available at any finer temporal resolution during this study. While the simulated rainfall patterns during each of the 3-h intervals for November during the three years are slightly different, the diurnal cycles are quite similar. For example, the diurnal cycles of rainfall over all four quadrants are characterized by nocturnal peaks (between midnight and early morning hours), with rainfall drastically diminishing over the entire lake surface thereafter.

These results are consistent with those of previous studies by Datta (1981), Ba and Nicholson (1998), and Song et al. (2002), all of which showed that the diurnal cycle of rainfall over a limited sample of lake island

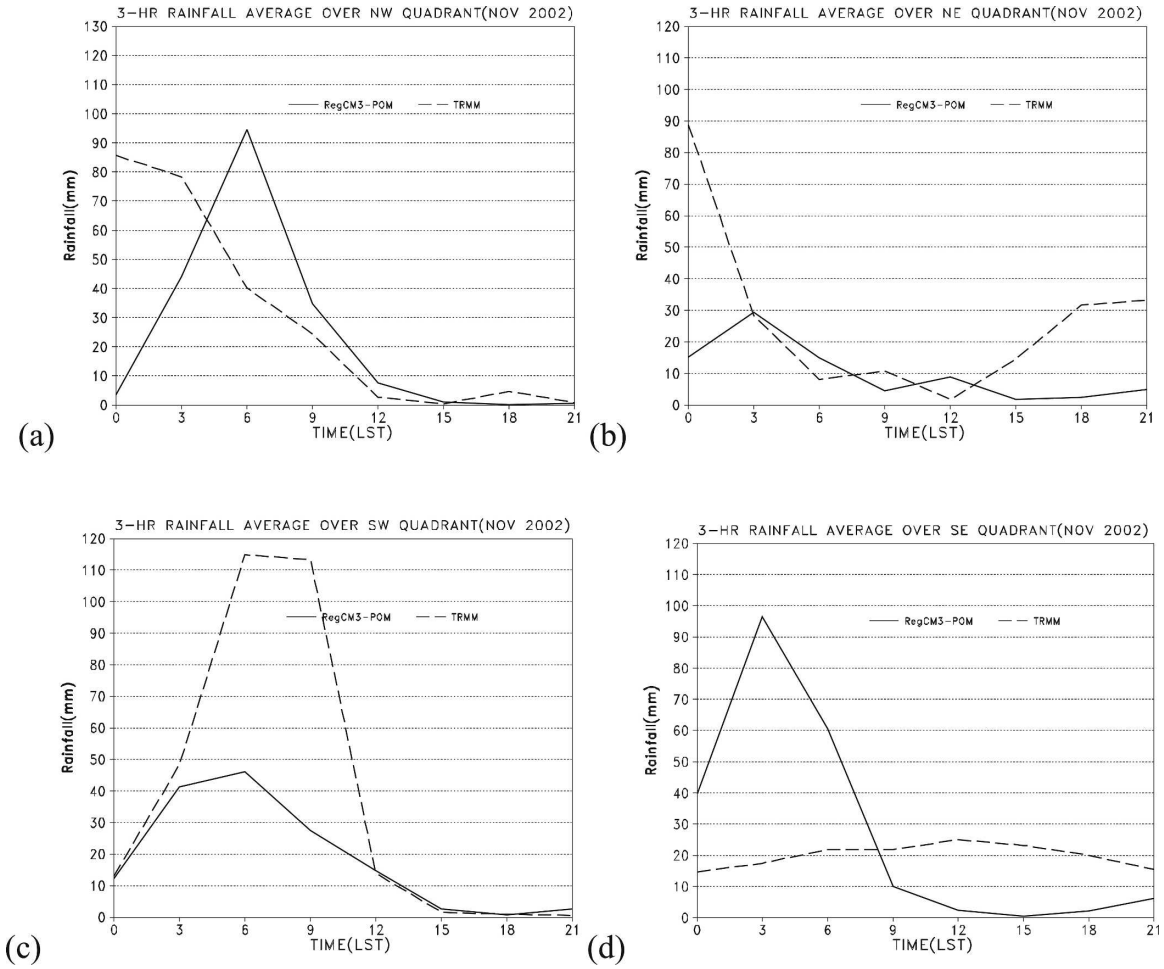

FIG. 9. Same as in Fig. 7, but for November 2002.

stations and lakeshore stations over different parts of the lake is characterized by nocturnal peaks. Evidently, the overlake rainfall is mainly experienced during late night into early morning hours when there is uplift or rising motion over the relatively warmer lake surface associated with land breeze circulation. During the day, there is sinking motion and flow divergence (Fig. 6) over the lake surface due to reversal in the thermal gradient between the lake and surrounding land areas (lake breeze circulation). The lowest rainfall amounts are simulated over the SE quadrants for all three years. The 850-hPa (~300 m above lake surface elevation) simulated mean temperature gradient between the lake and land at 15 LST is in the order of 6°C, while at 3 LST it is much weaker, about 3.5°C. This could be due to the fact that nocturnal convection leads to rain-cooled air over the lake, which minimizes the lake–land temperature gradient.

It is evident from the simulated results that there is reasonable agreement between the model and TRMM estimates over southwestern and northwestern quadrants (Figs. 7c, 8c, and 9c) for all the November months in 1998, 2000, and 2002. At the same time, the simulated diurnal cycle over the southeastern sector of the lake is not consistent with TRMM estimates during all three years. Overall, the simulated diurnal rainfall variability is relatively more consistent with TRMM satellite estimates in 2000 (near-normal season) than during the 1998 and 2002 seasons. This is possibly a manifestation that large-scale climate anomalies (El Niño and La Niña events) are superimposed even in the diurnal variability of the lake basin climate and weather patterns.

c. Contribution of large-scale moisture to the lake basin rainfall variability

A suite of sensitivity experiments (described in section 2c) were performed by systematically reducing the amount of large-scale moisture advected into the lake basin through the four lateral boundaries. Figure 10 shows the response of the simulated lake basin rainfall

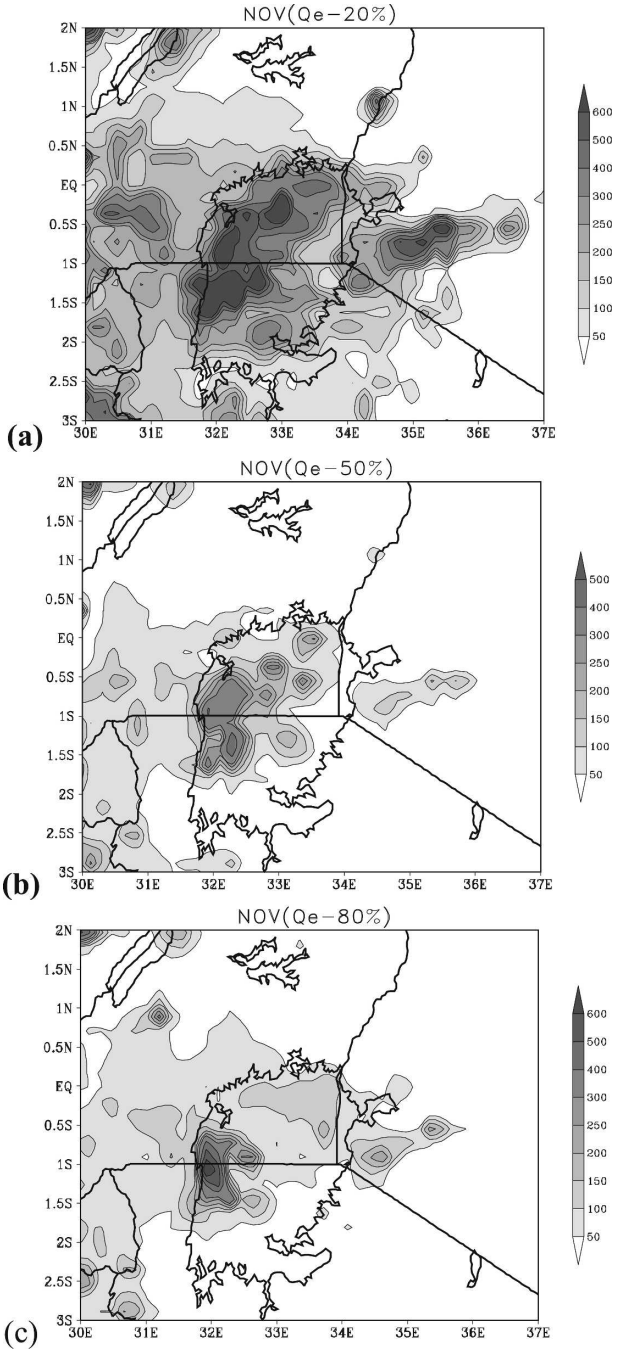

FIG. 10. Simulated rainfall (mm) over Lake Victoria basin with large moisture through the eastern boundary reduced by (a) 20%, (b) 50%, and (c) 80%.

to changes in large-scale moisture advected into the interior domain via the eastern lateral boundary located across the western Indian Ocean. This experiment was specifically designed to attempt to quantify some of the evidence shown in previous observational/empirical studies that rainfall variability over eastern

TABLE 1. Response of lake basin rainfall to large-scale moisture anomaly.

Expt	Qw-50	Qe-50	Qn-50	Qs-50	Qa-50	CTRL
Overlake rainfall (mm)	338.1	120.2	321.2	315.3	120.9	328.4
Δ%	+3	−63	−2.3	−3.9	−63	0

Africa during the short rains season is significantly influenced by the SST gradients (moisture anomalies) over the equatorial Indian Ocean (Saji et al. 1999; Mutai and Ward 2000). Figures 10a–c show simulated rainfall variability in November 2000 when lateral boundary moisture forcing was reduced by 20%, 50%, and 80%, respectively. To avoid any instabilities/inconsistencies in both the dynamics and physics of the model and uncertainties in interpreting the model results, the lateral boundary moisture (mixing ratio) was reduced (dried) before being interpolated onto the model grids in the interior domain.

It is evident from our results that the simulated rainfall amount reduces dramatically as the amount of moisture entering the interior domain through the eastern boundary is systematically reduced. As would be expected, it is also apparent that the eastern side of the lake exhibits more sensitivity to the moisture reduction (changes). This is also consistent with the fact that the prevailing monsoonal flow over the lake basin is easterly most of the year. When large-scale moisture over the eastern boundary is reduced by half, the corresponding decrease in the simulated rainfall compared to the control was quite dramatic over the entire lake basin. The overlake averaged rainfall also generally reduces significantly (by about 50%) compared with the control (Table 1). With the large-scale moisture entering the interior domain (lake basin) through the eastern boundary reduced by 80% (Fig. 10c), the reduction in the simulated rainfall amount is quite dramatic over the entire lake basin, except over a small region in the western-to-southwestern sector of the lake surface.

When large-scale moisture entering the western boundary of our domain is reduced by 50% (Qw-50; Fig. 11b), the corresponding reduction in the simulated rainfall is negligible compared to the control experiment. However, a rather surprising feature is the slight increase in the amount of area-averaged simulated rainfall over the lake surface, which possibly indicates the nonlinear response and feedback between the local and large-scale moisture sources over the lake basin. Similarly, when large-scale moisture entering the southern boundary is reduced by 50% (Qs-50; Fig. 11c), the re-

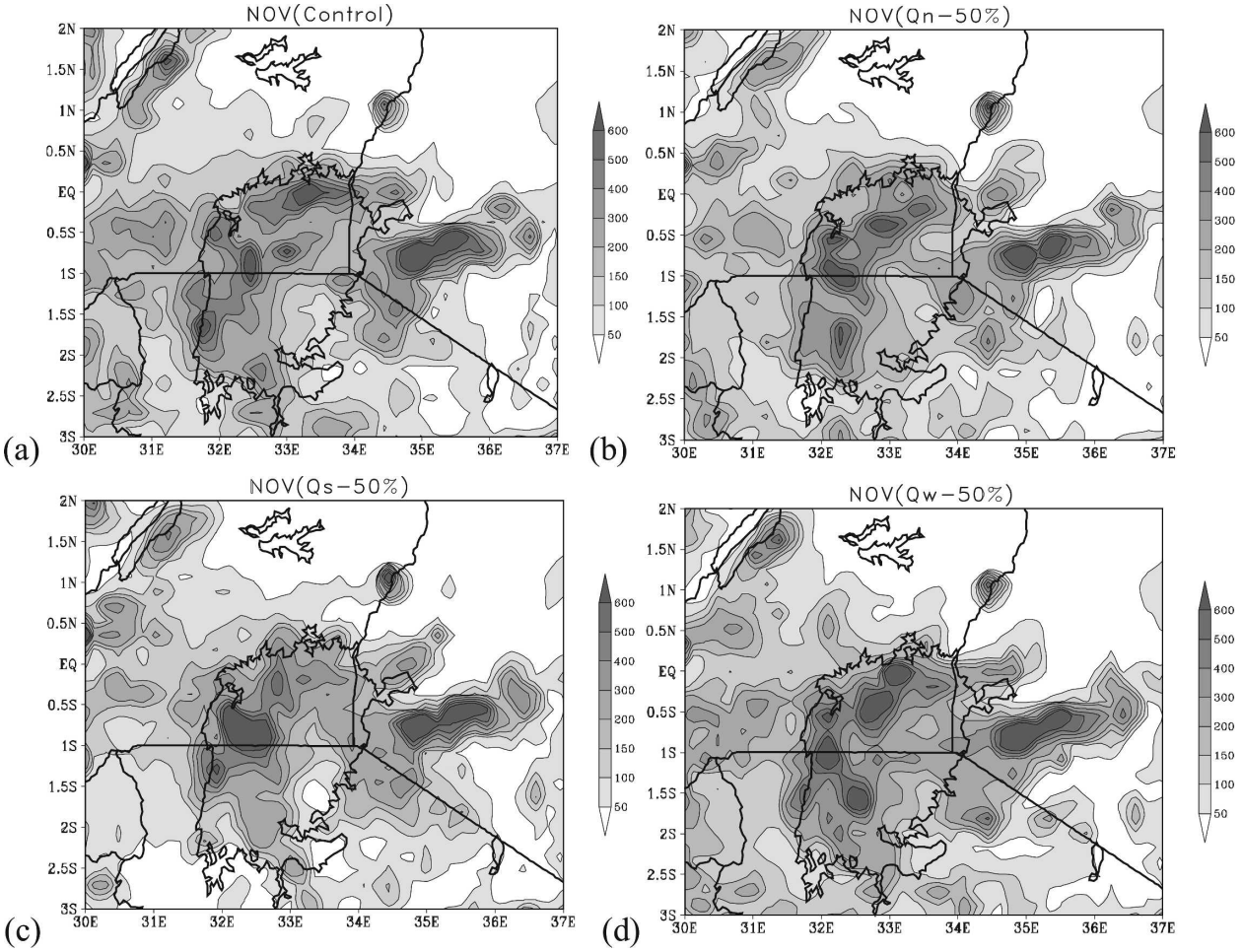

FIG. 11. Simulated monthly mean rainfall over the lake basin in November (1998–2002) with large-scale moisture advected across different boundaries reduced by 50% in the (a) control, (b) northern boundary, (c) southern boundary, and (d) western boundary experiments.

duction in the total overlake rainfall is negligible (~4%). Our results also show that the simulated rainfall averaged over the lake surface in the Qn-50 experiment is only less than the control by about 3%, almost similar to the Qs-50 experiment (Table 1), although the reduction in the simulated rainfall amount seems to be confined over the northern parts of the lake catchment. However, the dominant impact of the large-scale moisture entering the eastern boundary is demonstrated in the results of Qa-50 (i.e., large-scale moisture via all four lateral boundaries is reduced by 50%; Table 1), where the corresponding changes in the rainfall pattern and amounts over the entire basin are more similar to those of the Qe-50 experiment (Fig. 10b).

d. Effects of lower-boundary forcing on Lake Victoria basin climate variability

To isolate and understand some of the mechanisms associated with interactions between topographic and lake-induced circulations and their impacts on lake basin climate variability, we performed three experiments where

(i) the high terrain all around the lake basin was smoothed leaving maximum terrain height at 1300 m (TPALL), which is just above the lake surface elevation;
(ii) only the terrain between the lake and Indian Ocean (TPEA) was smoothed, as in (i);
(iii) effects of changes in the lake surface characteristics on lake basin climate were investigated by replacing the lake surface with marsh/swamp (LBOG).

Our analysis of the response/sensitivity of lake basin climate to the changes in lower-boundary forcing (described in the list above) is based mainly on simulated rainfall and vertical (omega) velocity. Unfortunately, while the simulated overlake rainfall in the control run is compared with TRMM satellite estimates, no obser-

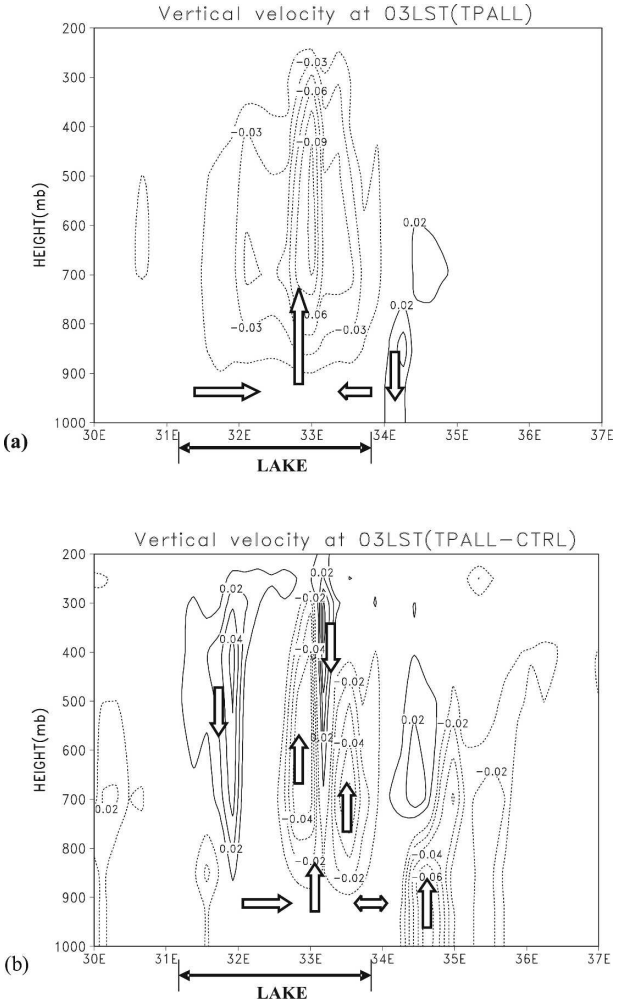

FIG. 12. Vertical (omega) velocity profiles in the TPALLexperiments at 0300 LST for (a) TPALL and (b) TPALL − CTRL.

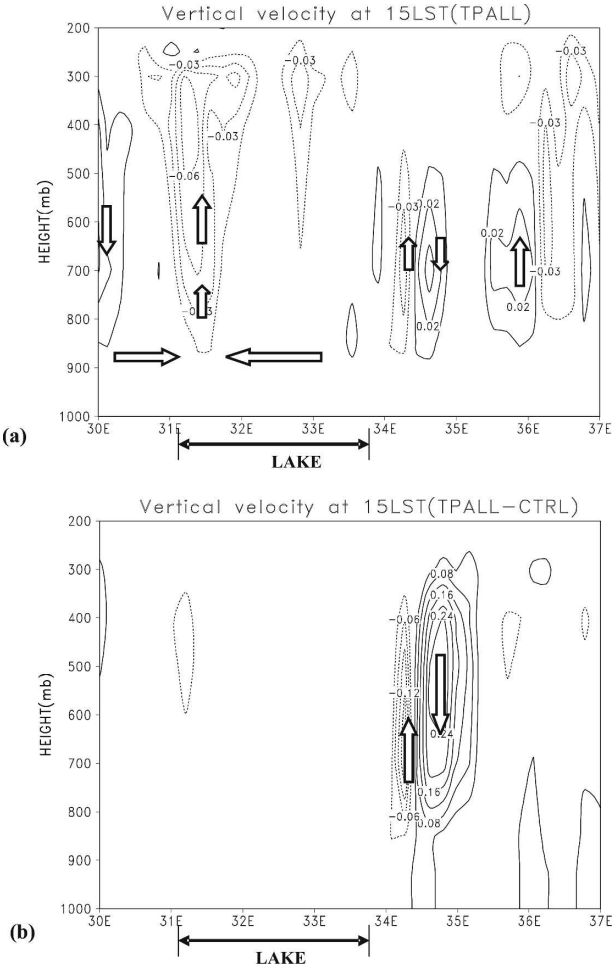

FIG. 13. Same as Fig. 12, but at 1500 LST.

vations of the vertical velocity or related fields were available during this study to evaluate the simulated fields. Figures 12a,b show the simulated mean vertical velocity (November 2000) at 3 LST and 15 LST in the TPALL experiment. Figure 12a shows that the western sector of the lake is characterized by strong upward motion, with maximum vertical velocity located approximately over the center of the lake (33°E). The rising motion extends over a very deep column, from the lake surface (~900 hPa) to around 300 hPa. This upward motion is apparently associated with very deep convection and produces significant amounts of rainfall over the western sector as consistent with the control simulations shown in Fig. 3. The eastern side of the lake is, however, characterized by net subsidence. This flow pattern is consistent with the expected diurnal circulation and rainfall variability over the lake basin associated with lake- and land- breeze circulations (Figs. 6, 7, 8, and 9). Nevertheless, the region of the strongest rising motion is located over the center of the lake. Thus in the absence of strong downslope winds over the highlands east of the lake (due to smoothed terrain), the eastern branch of the land breeze is weakened and does not extend farther to the west of the lake surface. Conversely, the western branch becomes relatively stronger and extends more offshore into the interior of the lake than in the control. This is consistent with the vertical velocity difference (TPALL − CTRL) presented in Fig. 12b that shows net subsidence over the western sector of the lake and net uplift over the center of the lake.

The likely mechanism that contributes to the above vertical flow characteristics can be explained as follows: Smooth topography east of the lake leads to weaker downslope flow. With weaker downslope winds, less cooler air from the mountain tops is transported down the valley to help in enhancing the lake–land thermal gradient (i.e., weaker land breeze circulation) as compared to the control. When the eastern branch of the

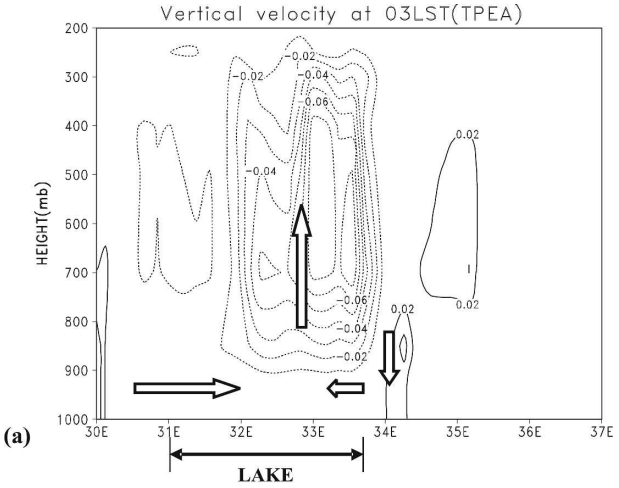

FIG. 14. Same as Fig. 12, but for TPEA experiment.

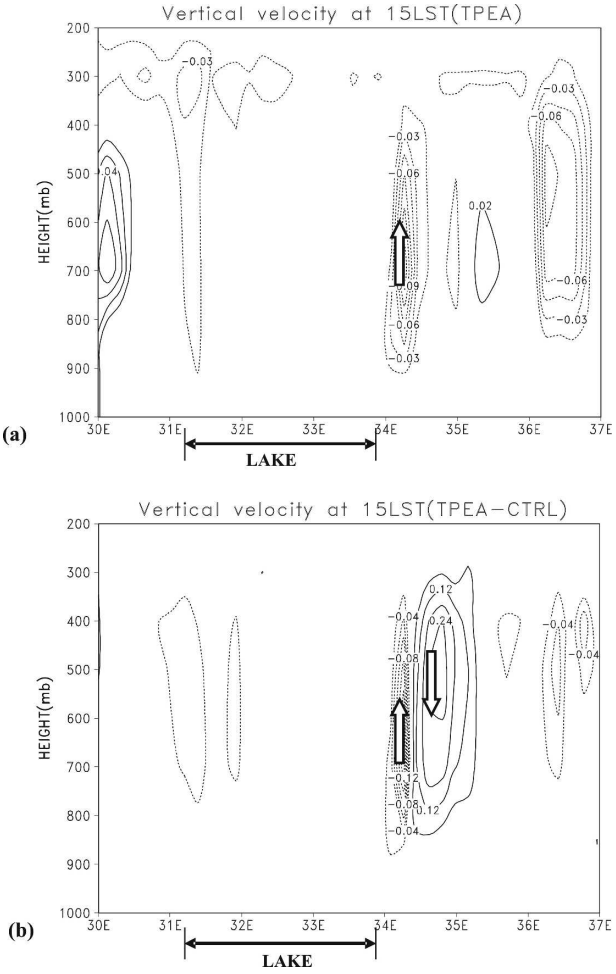

FIG. 15. Same as Fig. 12, but for TPEA experiment at 1500 LST.

land breeze is relatively weaker than normal, the western branch of the nocturnal circulation then becomes relatively stronger and penetrates into the interior of the lake as shown in Fig. 12a.

In the late afternoon (Fig. 13a), smooth topography east of the lake catchment (TPALL) results in much weaker upward motion. The rising motion (collocated with the apparent lake breeze front) is also located around 34.5°E, close to the lakeshore. A rather unexpected feature is the subsidence over the highlands farther east of the lake (around 35°E). This possibly suggests that the late afternoon thunderstorms experienced over the NKK highlands (located about 70 km east of Lake Victoria; Fig. 1) are significantly influenced by a combination of orographic lifting of the moisture embedded in the prevailing monsoon circulations and moisture transport from Lake Victoria via lake breeze circulation. The vertical velocity difference (TPALL − CTRL) in Fig. 13b also show that there is net subsidence over the highlands east of the lake (around 35°E) and net upward motion along the eastern lakeshore.

In the early morning (3 LST; Fig. 14a), when the nocturnal (land breeze) circulation is expected to be at its peak, the TPEA simulations show rising motion over the center of the lake. However, the upward motion is weak (only reaching a maximum of about 0.1 m s^{-1} at the center of the lake). Also, the subsidence (sinking motion) to the east of the lake is very weak. The difference between TPEA and CTRL experiments (Fig. 14b) indicates net upward motion over the center of the lake and net subsidence (sinking motion) over the western rim of the lake. The results also suggest that the horizontal branch of land breeze circulation at the surface originating from the western side of the lake is relatively stronger than it is in the control run. Two possible physical mechanisms may be responsible for the simulated vertical velocity pattern. First, the steep topography east of the lake influences the strength of

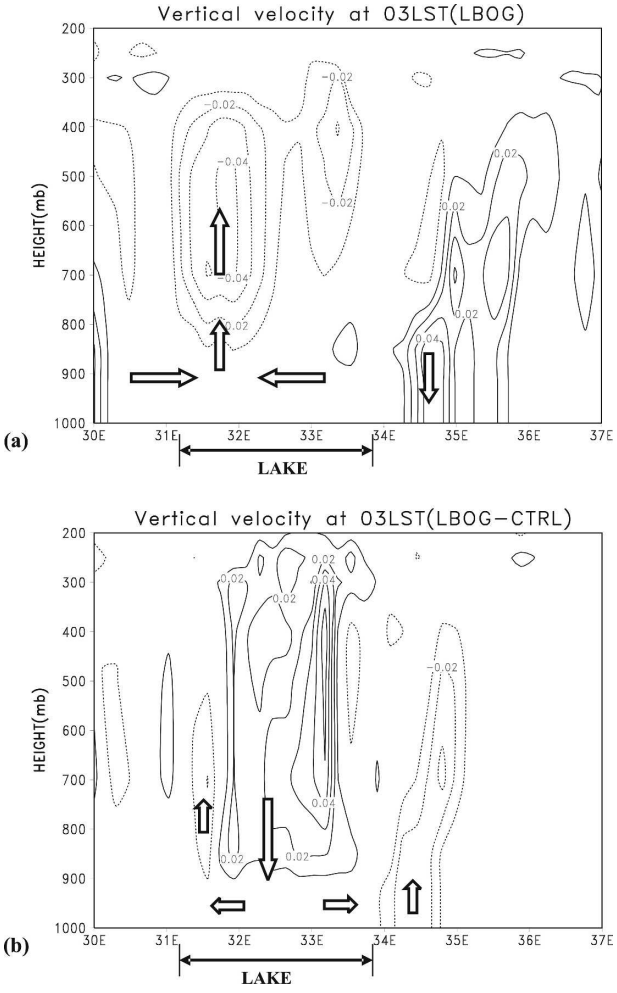

FIG. 16. Same as Fig. 12, but for LBOG experiment.

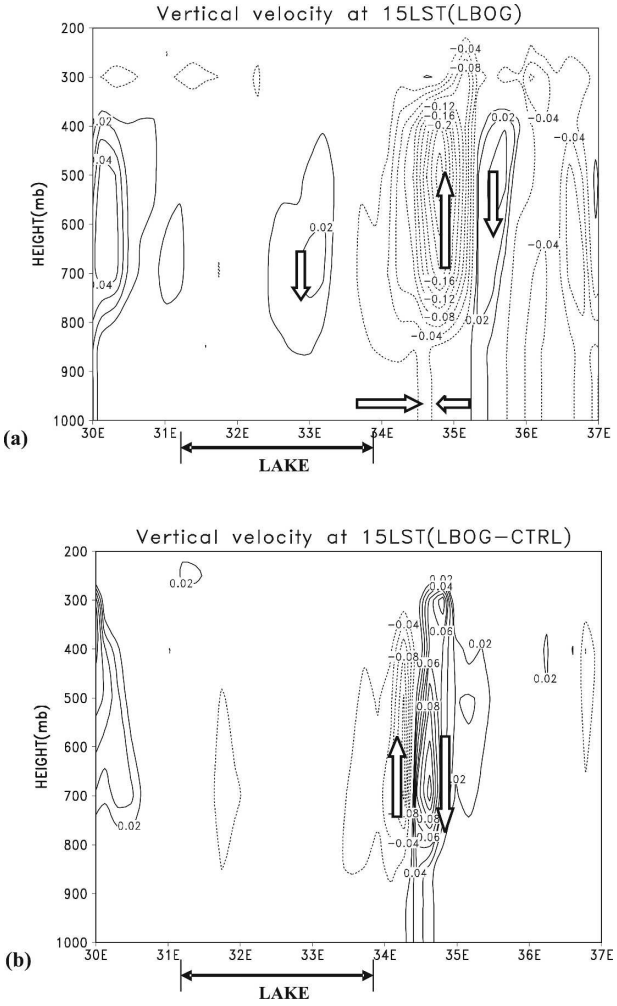

FIG. 17. Same as Fig. 12, but for LBOG experiment at 1500 LST.

the eastern branch of the nocturnal circulation (land breeze). The cold downslope (katabatic) flow helps to decrease the surrounding air temperature as it speeds down the topography. This enhances the land–lake thermal gradient and in turn intensifies the land breeze circulation.

In the late afternoon (Fig. 15a), the ascending motion to east of the lake is relatively weaker and more confined to the shoreline (34°E) in the TPEA compared with the control run. The difference between the vertical velocities in TPEA − CTRL shown in Fig. 15b also indicates that there is net upward motion confined along the eastern rim of the lake and net subsidence (sinking motion) located slightly inland (between 34.5° and 35.5°E). Possible mechanisms associated with the differences in vertical motion between TPEA and CTRL simulations could be explained as follows: The reduced terrain height over the highlands east of the lake results in weak upward motion (in the absence of elevated heating). However, given the relatively weak wind speeds over the lake (westerly winds), the lake breeze front does not appear to extend farther inland east of the lake as in the control but remains confined along the lake perimeter. Furthermore, the lower the terrain height over the east of the lake, the more penetrative the prevailing easterlies into the lake basin, leading to flow convergence closer to the lakeshore as opposed to the control run. This implies that the elevated heating over the NNK highlands (Fig. 1) mostly triggers strong upslope flow during the day. This may play two major roles with respect to the strength, horizontal extent, and convective activity associated with the lake breeze circulation. First, the elevated heating over the highlands to the east of the lake triggers strong upslope flow, which then creates favorable conditions for entraining (inducing) flow from the lake and thus makes the horizontal branch of the lake breeze extend farther inland than it would otherwise be. However,

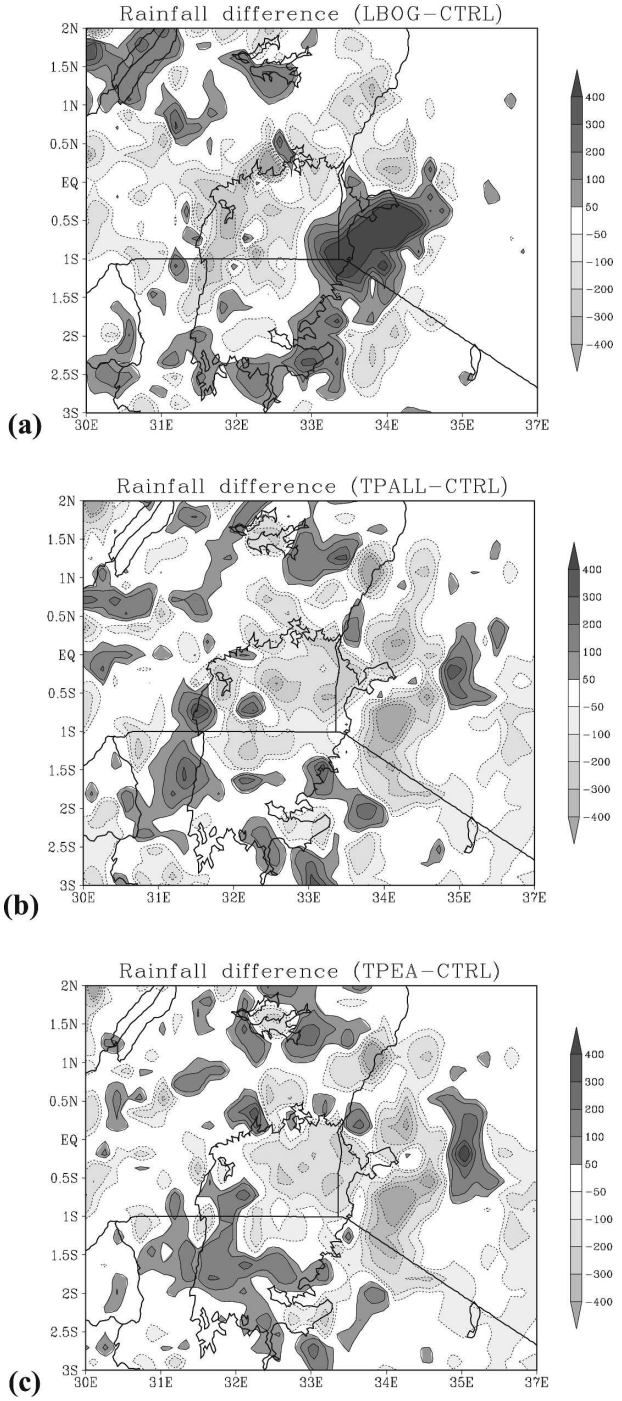

FIG. 18. Sensitivity of Lake Victoria basin rainfall to surface boundary conditions for (a) LBOG − CTRL, (b) TPALL − CTRL, and (c) TPEA − CTRL in November 2000.

this still depends on the magnitude of the lake–land thermal gradient. Second, due to orographic lifting and its influence on the horizontal extent of lake breeze explained above, the region of strong vertical motion (lake breeze front) forms more inland in the control case than in the case with less steep topography that does not generate strong upslope winds.

e. Effects of changes in the physical characteristics of Lake Victoria on basinwide climate variability

The impact of changes in the lake surface conditions on the basinwide rainfall variability is examined by replacing the lake with bog/marsh (swamp; LBOG experiment). Given the recent invasion of Lake Victoria by the water hyacinth weed, this experiment tests a realistic scenario of the lake surface conditions.

The simulated response of the lake basin circulation at 0300 LST is characterized by weak upward motion over the western sector of the lake (Fig. 16a) that extends from around the lake surface to about a 400-hPa level. On the other hand, a relatively strong subsidence is simulated to the east of the lake, extending from the surface up to around 500 hPa. The LBOG minus CTRL simulations show a net sinking motion over the center of the lake (Fig. 16b) and extend over a very deep layer (900–200 hPa). This is consistent with the fact that in the LBOG experiment, less heat is retained during the day compared to the CTRL experiment because of changes in surface albedo, surface roughness, and thermal capacity. Consequently, at night, the lake–land thermal contrast that triggers the nocturnal circulation is significantly suppressed. Hence, the nocturnal circulation that is normally characterized by convergence over the western sector of the lake (control) is suppressed remarkably.

In the late afternoon, the upward motion to the east of the lake is enhanced in the LBOG experiment (Fig. 17a) compared to the control simulations. This is possibly due to the fact that unlike the dynamic lake, bog/marsh conditions trigger stronger evaporation since they do not retain most of the heat received from solar radiation. This leads to stronger evaporative cooling that consequently creates a sufficient land–lake thermal gradient, in turn driving a lake-breeze-like circulation. This is consistent with results (see Fig. 20) showing that the mean monthly evapotranspiration (mm) averaged over the lake surface in LBOG is less than in CTRL by almost 40 mm over the western sector of the lake. This can be attributed to the overall changes in the surface roughness, albedo, and thermal capacity of the lake (marsh).

f. Anomalous rainfall response to lower-boundary forcing

The simulated rainfall differences between LBOG, TPALL, TPEA, and CTRL in November 2000 are shown in Fig. 18. In Fig. 18a, the LBOG minus CTRL

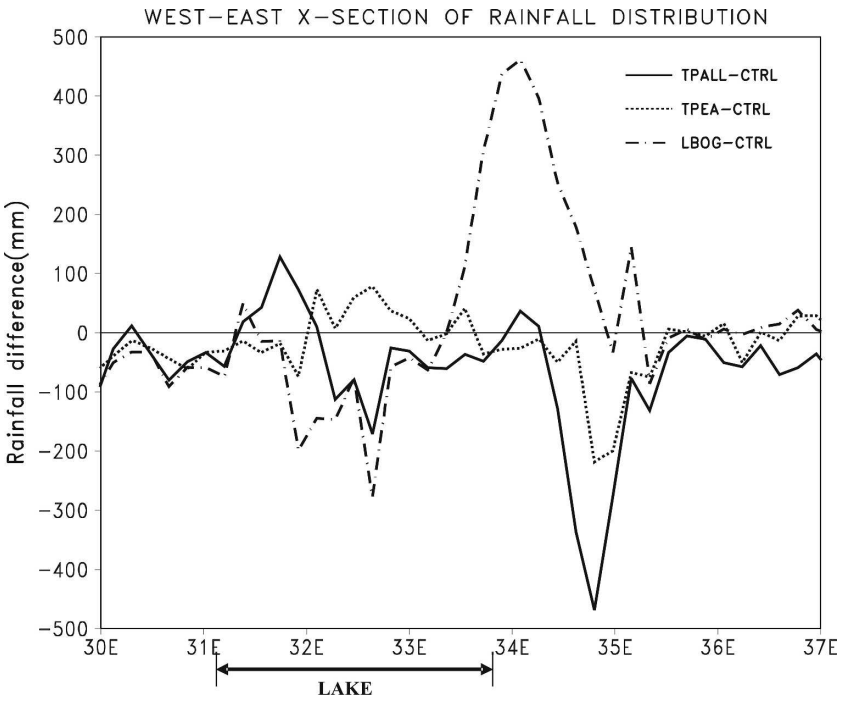

FIG. 19. Differences in the distribution of simulated rainfall across the Lake Victoria basin between CTRL and TPALL, TPEA, and LBOG experiments.

is characterized by rainfall deficit over the western half of the lake and rainfall surplus over the eastern shoreline of the lake. However, immediately outside the lake perimeter to the east, there is little or no difference between the LBOG and CTRL simulations. The most striking feature is that over the immediate land areas east of the lake, the simulated amount of rainfall is almost twice the amount in the control simulation.

Three possible mechanisms could be responsible for the increase (decrease) in the rainfall amount simulated over the eastern (western) shoreline when the lake is replaced with bog/marsh. First, the significant reduction in the simulated rainfall over the western sector could be attributed to the anomalous subsidence over the lake surface associated with the nocturnal circulation pattern shown in Fig. 16. The subsidence of motion over the lake during late night through early morning hours could be due to the fact that the bog/marsh has relatively lower thermal capacity. This means that the "lake" will cool faster at night, significantly suppressing nocturnal circulation as a consequence of a weaker land–lake thermal gradient.

The second mechanism may be attributed to increased evaporation over the lake surface during the day. This leads to evaporative cooling, thus creating a sufficient thermal gradient with the surrounding land areas, which in turn drives a relatively strong circulation (lake breeze like) directed toward the warmer surrounding. However, this circulation is not as strong as the lake breeze circulation simulated in the control and thus has limited horizontal extent. This explains why the approximate location of the lake breeze front (also collocated with the region of maximum precipitation) is close to the eastern shoreline in the LBOG simulations, while in the CTRL it is located farther inland.

The third mechanism that may limit (enhance) the penetration of the horizontal branch of the lake breeze circulation inland in the LBOG experiment is due to increased (reduced) nocturnal convection. Intense nocturnal convection leads to more precipitation over the lake surface (western sector), thus triggering outflow from the lake due to the rain-cooled overlake air. This in return determines how far the horizontal branch of the lake breeze circulation will penetrate inland in the late afternoon.

It is also evident in Figs. 18b,c that when the maximum terrain height all around Lake Victoria is smoothed (TPALL), less rainfall is simulated over the eastern border and northern and northwestern sectors of the lake compared to the control. On the other hand, relatively more rainfall is simulated over the western border of the lake, but confined just along the rim of the lake (32°E). As shown earlier in section 3c, the eastern sides of the lake catchment tend to benefit a lot from moisture entering the lake basin through the eastern lateral boundary (western Indian Ocean). How-

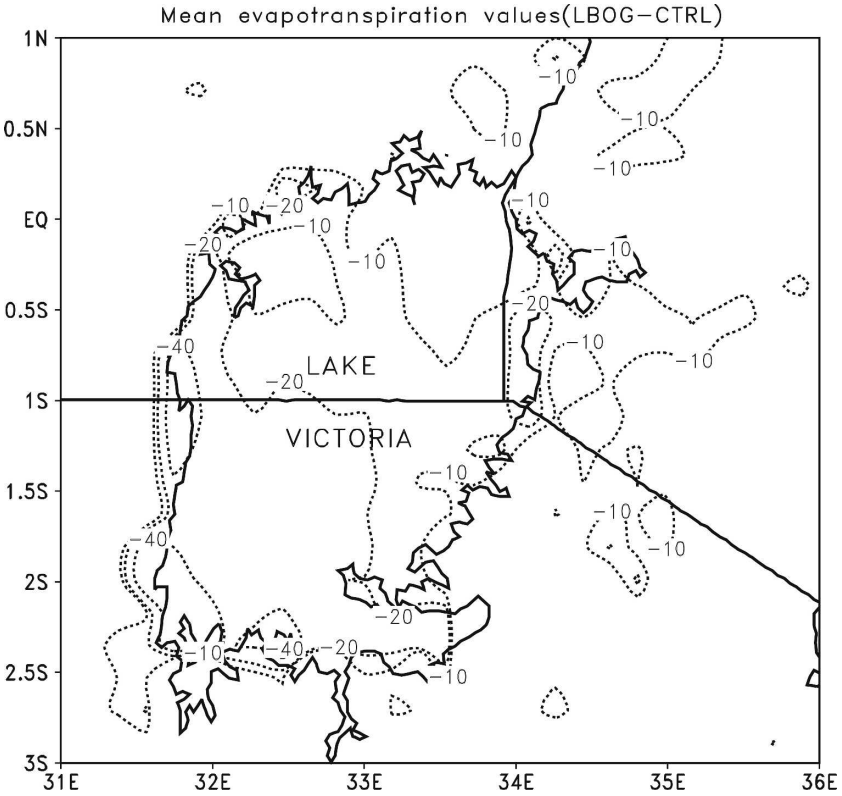

FIG. 20. Difference in mean evapotranspiration rate (mm) in LBOG − CTRL in November 2000.

ever, it is also evident from the vertical velocity fields shown earlier in Figs. 11–14 that orographic lifting over the eastern side of the lake may also help to organize and enhance convection. The mountain breeze (upslope winds) to the east of the lake creates favorable conditions for the interactions between large-scale moisture transported via the prevailing easterly monsoons and moisture from the lake transported via the land–lake breeze circulations. This interaction is significantly suppressed when the terrain height is reduced. However, over the western sector of the lake, the reduced terrain height to the east of the lake basin results in relatively more large-scale moisture penetrating into the lake basin, especially during nocturnal land breeze circulations, and thus enhances precipitation over the western half of the lake.

The rainfall anomalies associated with land surface forcing are also exhibited in the horizontal (west–east) cross section of rainfall distribution over the lake basin (Fig. 19). It is apparent that the steep topography to the east of the lake does influence the amount of rainfall simulated over the entire basin, whereas the topography to the west side of the lake only imposes a negligible impact on the diurnal variability of rainfall over the lake basin, at least during the short rains season. Comparisons among LBOG, TPEA, TPALL, and CTRL confirm that lake surface conditions significantly influence the distribution and pattern over the lake basin. This is also manifested in the simulated evapotranspiration differences between LBOG and CTRL runs (Fig. 20), where it can be seen that the mean monthly evapotranspiration (mm) averaged over the lake surface in LBOG is less than CTRL by almost 40 mm over the western sector of the lake. This can be attributed to the overall changes in the surface roughness, albedo, and thermal capacity of the lake (marsh). Furthermore, though the LBOG case experiences stronger evaporation during the day, the nighttime component is significantly suppressed. Thus, on the mean, the evapotranspiration in the control is relatively larger than in the LBOG (Fig. 20).

4. Summary and conclusions

In this study, the downscaling ability of a fully coupled RegCM3–POM system to reproduce the multiscale variability of Lake Victoria basin climate and the associated physical mechanisms has been demon-

strated. In general, the mean monthly rainfall simulated over the lake basin, particularly over the lake surface, is shown to reasonably agree with the satellite estimates (TRMM data). The simulated diurnal cycle of rainfall over the four quadrants of the lake shows a coherent pattern with the TRMM diurnal rainfall fluctuations. Rainfall peaks occur between midnight and early morning hours, and thereafter, a general decline in both simulated and TRMM rainfall is witnessed over the lake and areas within the immediate catchment. However, the simulated diurnal cycle tends to have midnight through early morning rainfall peak a little earlier than in the TRMM estimates.

Two mechanisms can be inferred from our model results regarding interactions between topographic and lake-induced circulations and the consequent impact on lake basin rainfall variability:

(i) The steep topography east of Lake Victoria generates very strong downslope (katabatic) winds at night since the air over the mountain top is relatively colder than the air down the valley. As the colder air from the mountain tops mixes with air down the valley and air over land areas adjacent to the lake, the thermal gradient between the land surface and the lake is enhanced. Consequently, a relatively stronger land breeze circulation is generated. The stronger the land breeze circulation, the more favorable it is for strong convection and precipitation to develop over the central and western sectors of the lake. The opposite is the case when the terrain height is smoothed, as is also clearly evident in our simulations.
(ii) The horizontal extent of the late afternoon lake breeze circulation is also affected by steep topography east of the lake. Due to high elevation, the mountain tops heat faster during the day than the surroundings. This creates a thermal low that in turn induces significant upslope (anabatic) winds on both sides of the mountain. The stronger the upslope flow on the lee side of the mountains east of the lake, the more this flow would tend to pull (entrain) the lake breeze front farther inland. Hence, when the terrain height is reduced/smoothed, the horizontal extent of the lake breeze circulation also reduces. This leads to significant reduction in the simulated afternoon rainfall associated with the lake breeze circulation in areas far away from the lake. Thus, the simulated rainfall tends to be confined along the eastern shoreline, but does not extend farther inland compared to the control simulation.

The simulated response of the nocturnal circulation to changes in the physical characteristics of the lake (i.e., replacing lake with marsh) is characterized by weak upward motion over the western sector of the lake. This is consistent with the fact that when the lake is replaced with marsh (or water hyacinth), it retains less heat during the day due to changes in surface albedo, surface roughness, and thermal capacity. Consequently, at night, the lake–land thermal contrast that triggers the nocturnal circulation is significantly suppressed. Conversely, in the late afternoon, the upward motion to the east of the lake (near the shore) is more enhanced compared to the control simulations, possibly due to the fact that the marsh conditions trigger stronger evaporation since they do not retain most of the heat received from solar radiation. This leads to stronger evaporative cooling that consequently creates a sufficient land–lake thermal gradient, in turn driving a lake-breeze-like circulation.

The apparent role of the large-scale moisture transported via the prevailing easterly monsoons in enhancing precipitation over the lake basin is also clearly manifested in our simulations. This is evident in the simulated rainfall patterns and by the amounts in the runs with large-scale moisture entering the four lateral boundaries of the interior domain (Lake Victoria basin) systematically reducing or increasing. A more striking result is that large-scale moisture advected through the eastern boundary (located across the equatorial western Indian Ocean) enhances overlake rainfall, especially over the surrounding land areas to the east and southeast of the lake. However, a rather surprising result is that there is negligible influence on the basinwide (particularly overlake) rainfall variability because of changes in large-scale moisture entering the lake basin domain through the western, northern, and southern boundaries.

Acknowledgments. The valuable comments made by Jared Bowden, Robert Mera, Neil Davis, and Baris Onol on the original manuscript are highly appreciated. We would also like to thank the three anonymous reviewers for their insightful comments that led to significant improvement of the original manuscript. This research was supported by NSF Grant ATM-0438116. The model experiments were performed on the National Center for Atmospheric Research (NCAR) supercomputers and at the North Carolina State University High Performance Center. NCAR is sponsored by the National Science Foundation.

REFERENCES

Anyah, R. O., 2005: Modeling the variability of the climate system over Lake Victoria Basin. Ph.D. dissertation, North Carolina

State University, 287 pp. [Available online at http://www.lib.ncsu.edu/theses/available/etd-07202005-123806/.]

——, and F. H. M. Semazzi, 2004: Simulation of the response of Lake Victoria basin climate to lake surface temperatures. *Theor. Appl. Climatol.,* **79,** 55–69.

Anyamba, E. K., 1984: Some aspects of the origin of rainfall deficiency in East Africa. *Proc. Regional Scientific Conf. on GATE, WAMEX and Tropical Meteorology,* Dakar, Senegal, WMO, 110–112.

Asnani, G. C., 1993: *Tropical Meteorology.* Vols. 1 and 2. Indian Institute of Tropical Meteorology, 1012 pp.

Ba, M. B., and S. E. Nicholson, 1998: Analysis of convective activity and its relationship to rainfall over the Rift Valley Lakes of East Africa during 1983–90 using the meteosat infrared channel. *J. Appl. Meteor.,* **37,** 1250–1264.

Blumberg, A. F., and G. L. Mellor, 1987: A description of a three-dimensional coastal ocean model. *Three-Dimensional Coastal Ocean Models,* N. Heaps, Ed., Amer. Geophys. Union, 1–16.

Datta, R. R., 1981: Certain aspects of monsoonal precipitation dynamics over Lake Victoria. *Monsoon Dynamics,* J. Lighthill and R. P. Pearce, Eds., Cambridge University Press, 333–349.

Dickinson, R. E., A. Henderson-Sellers, and P. J. Kennedy, 1993: Biosphere–Atmosphere Transfer Scheme (BATS) version 1e as coupled to the NCAR Community Model. NCAR Tech. Note NCAR/TN-387+STR, 72 pp.

Fraedrich, K., 1972: A simple climatological model of the dynamics and energetics of the nocturnal circulation at Lake Victoria. *Quart. J. Roy. Meteor. Soc.,* **98,** 332–335.

Giorgi, F., M. R. Marinucci, and G. T. Bates, 1993a: Development of a second-generation regional climate model (RegCM2). Part I: Boundary-layer and radiative transfer processes. *Mon. Wea. Rev.,* **121,** 2794–2813.

——, ——, ——, and G. De Canio, 1993b: Development of a second-generation regional climate model (RegCM2). Part II: Convective processes and assimilation of lateral boundary conditions. *Mon. Wea. Rev.,* **121,** 2814–2832.

Hostetler, S., and F. Giorgi, 1992: Use of a regional atmospheric model to simulate lake-atmosphere feedbacks associated with Pleistocene Lakes Lahontan and Bonnevile. *Climate Dyn.,* **7,** 39–44.

——, G. T. Bates, and F. Giorgi, 1993: Interactive nesting of a lake thermal model within a regional climate model for climate studies. *J. Geophys. Res.,* **98,** 5045–5057.

Kalnay, E., and Coauthors, 1996: The NCEP/NCAR 40-Year Reanalysis Project. *Bull. Amer. Meteor. Soc.,* **77,** 437–471.

Kiehl, J. T., J. J. Hack, G. B. Bonan, B. A. Boville, B. P. Briegleb, D. L. Williamson, and P. J. Rasch, 1996: Description of the NCAR Community Climate Model (CCM3). NCAR Tech. Note NCAR/TN-420+STR, 152 pp.

Kummerow, C., and Coauthors, 2000: The status of the Tropical Rainfall Measuring Mission (TRMM) after two years in orbit. *J. Appl. Meteor.,* **39,** 1965–1982.

Laird, N. F., D. A. R. Kristovich, and J. E. Walsh, 2003a: Idealized model simulations examining the mesoscale structure of winter lake-effect circulations. *Mon. Wea. Rev.,* **131,** 206–221.

——, J. E. Walsh, and D. A. R. Kristovich, 2003b: Model simulations examining the relationships of lake-effect morphology to lake shape, wind direction, and wind speed. *Mon. Wea. Rev.,* **131,** 2102–2111.

McPherson, R. D., 1970: A numerical study of the effect of a coastal irregularity on a sea breeze. *J. Appl. Meteor.,* **9,** 767–777.

Mellor, G. L., 1991: An equation of state for numerical models of oceans and estuaries. *J. Atmos. Oceanic Technol.,* **8,** 609–611.

——, and T. Yamada, 1974: A hierarchy of turbulence closure models for planetary boundary layers. *J. Atmos. Sci.,* **31,** 1791–1806.

Mistry, V. V., and D. Conway, 2003: Remote forcing of East African rainfall and relationships with fluctuations in levels of Lake Victoria. *Int. J. Climatol.,* **23,** 67–89.

Mukabana, J. R., and R. A. Pielke, 1996: Investigating the influence of synoptic-scale monsoonal winds and mesoscale circulations on diurnal weather patterns over Kenya using a mesoscale numerical model. *Mon. Wea. Rev.,* **124,** 224–244.

Mutai, C. C., and M. N. Ward, 2000: East African rainfall and the tropical circulation/convection on intraseasonal to interannual time scales. *J. Climate,* **13,** 3915–3939.

Nicholson, S. E., 1996: A review of climate dynamics and climate variability in eastern Africa. *The Limnology, Climatology and Paleoclimatology of the East African Lakes,* T. C. Johnson and E. Odada, Eds., Gordon and Breach, 25–56.

——, 1998: Historical fluctuations of Lake Victoria and other lakes in the northern Rift Valley of East Africa. *Environmental Change and Response in East African Lakes,* J. T. Lehman, Ed., Kluwer, 7–35.

Ogallo, L. A., 1988: Relationship between seasonal rainfall in East Africa and Southern Oscillation. *Int. J. Climatol.,* **8,** 31–43.

Okeyo, A. E., 1987: The influence of Lake Victoria on the convective activities over the Kenya Highlands. *J. Meteor. Soc. Japan,* **65,** 689–695.

Pal, J. S., E. E. Small, and E. A. B. Eltahir, 2000: Simulation of regional-scale energy and water budgets: Representation of sub-grid scale cloud and precipitation processes in RegCM. *J. Geophys. Res.,* **105,** 29 579–29 594.

Saji, N. H., B. N. Goswami, P. N. Vinayachandran, and T. Yamagata, 1999: A dipole mode in the tropical Indian Ocean. *Nature,* **401,** 360–363.

Song, Y., F. H. M. Semazzi, and L. Xie, 2002: Development of a coupled regional climate simulation model for the Lake Victoria Basin. *The East African Great Lakes, Limnology, Paleolimnology and Biodiversity,* E. Odada and G. Olago, Eds., Gordon and Breach, 141–154.

——, ——, ——, and L. J. Ogallo, 2004: A coupled regional climate model for Lake Victoria basin of East Africa. *Int. J. Climatol.,* **24,** 57–75.

Sun, L., F. H. M. Semazzi, F. Giorgi, and L. A. Ogallo, 1999a: Application of the NCAR Regional Climate model to Eastern Africa. Part 1: Simulation of the short rains of 1988. *J. Geophys. Res.,* **104,** 6529–6548.

——, ——, ——, and ——, 1999b: Application of the NCAR Regional Climate model to Eastern Africa. Part 2: Simulation of interannual variability of short rains. *J. Geophys. Res.,* **104,** 6549–6562.

Sundqvist, H., E. Berge, and J. E. Krisjansson, 1989: Condensation and cloud parameterization studies with a mesoscale numerical weather prediction model. *Mon. Wea. Rev.,* **117,** 1641–1657.